SPHERIC Beijing International Workshop
17-20 October 2017

SPH Simulation of Couette Flow with Sinusoidally Moving Solid Boundary

Haiqiao Li **Hantao Liu**

The Lab. of Energy & Environment Engineering and Computational Fluid Dynamics,
North University of China, Taiyuan

Project supported by the National Natural Science Foundation of China (Grant No. 51476150).

Contents

Contents

1.1 Application of internal combustion engine

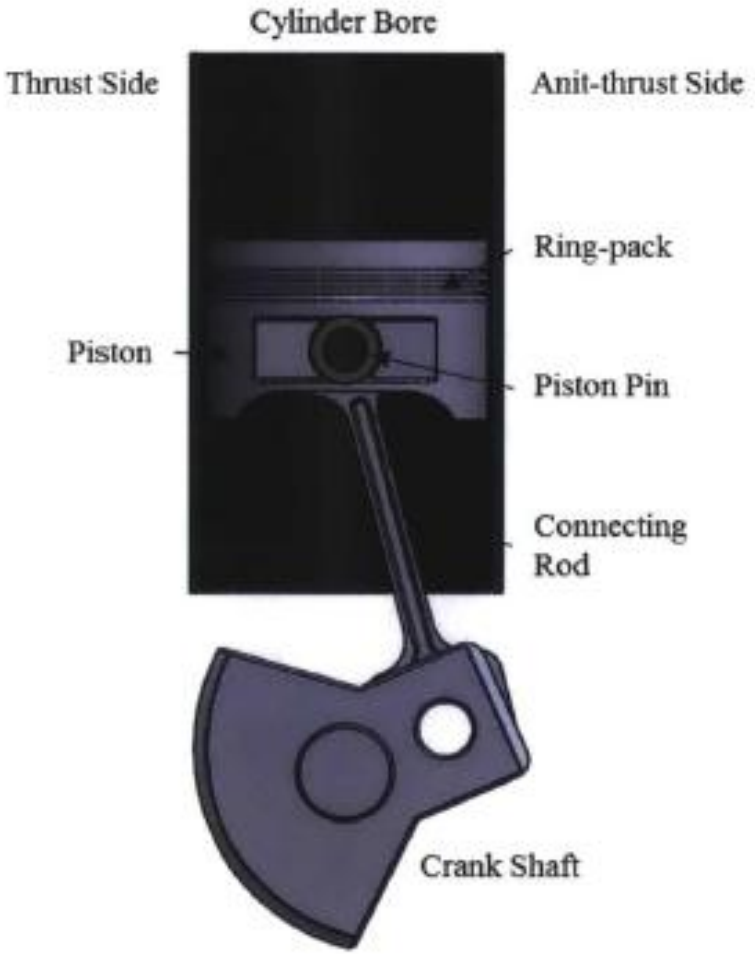

Fig. 1 internal combustion engine

1) transportation means
   Automobile
   Ship
   Submarine
   Motorcycle and so on
2) Power Generation
3) Agricultural Production
   Harvester
4) Industrial production
   Excavator
   Bulldozer
5) Military Industry
   Tank
   Armored Vehicle

……

1.2 mechanical friction in internal combustion engine

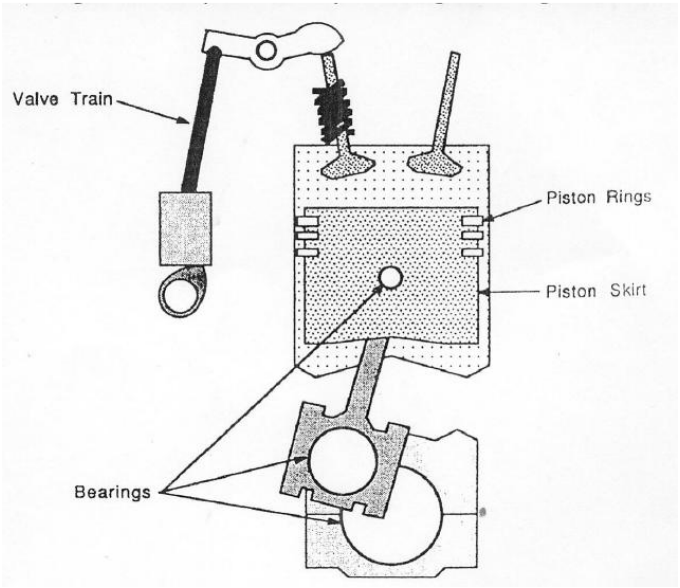

Fig. 2 Friction Pairs in internal combustion engine

★ 3 Main Friction Pairs

1) piston-liner

Piston Ring and Cylinder

piston skirt and Cylinder

2) Axis and Bearing

crank shaft and Bearing

connecting rod and Bearing

Piston Pin and Bearing

3) Valve System

cam tappet and rocker arm

Mechanical friction loss accounts for around 10% of the total energy in the fuel for a diesel engine.

40 - 55% of power cylinder system; 25 - 47% of piston.

28 - 45% of ring-pack; 18 - 33% of connecting-rod bearings.

friction loss generated at the piston skirt-liner interface can be about 40% of total piston assembly friction.

[1] Bai, D. (2012). Modeling piston skirt lubrication in internal combustion engines (Doctoral dissertation, Massachusetts Institute of Technology).

1.3 Phenomenon of Lubrication at Piston Skirt

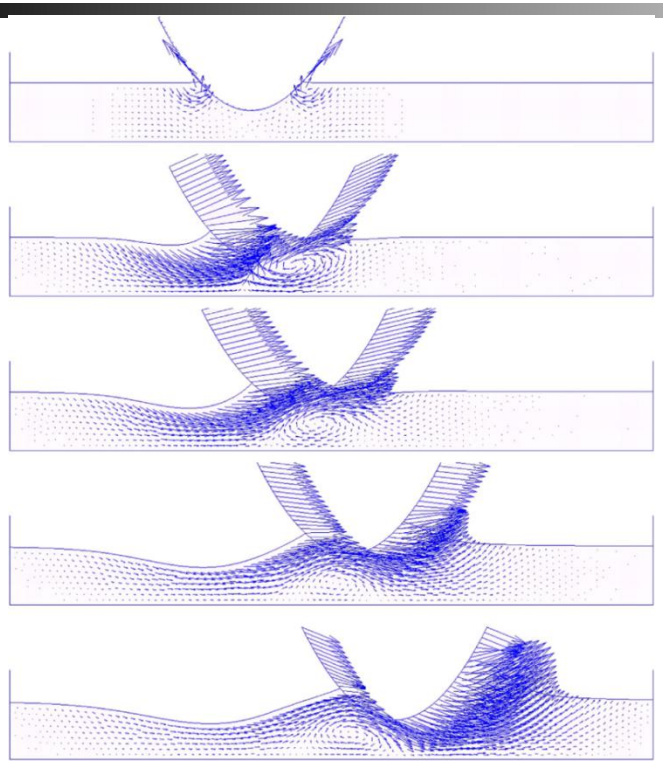

Fig. 3 oil scraper

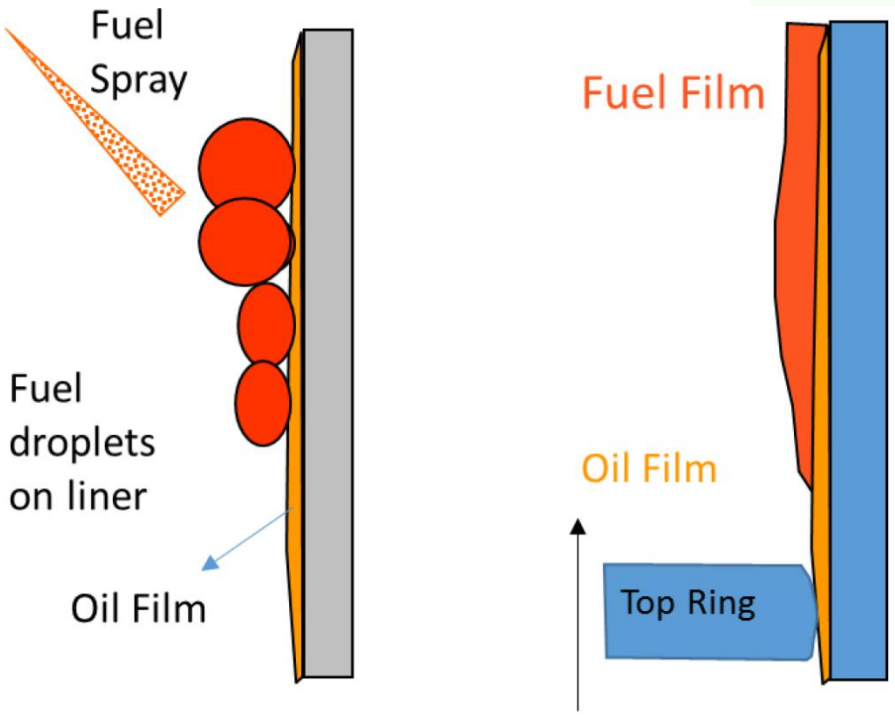

Fig. 4 Mixing of fuel and oil

The phenomenon of oil scrape, mixing of fuel and oil, oil supply etc. with free surface and large deformation. Simulation these phenomenon, which is the advantage of the SPH method.

[2] Liu, Y., Li, Y., & Tian, T. (2017). Development and Application of Ring-Pack Model Integrating Global and Local Processes. Part 2: Ring-Liner Lubrication. SAE International Journal of Engines, 10(2017-01-1047).
[3] Felter, C. L. (2008). Numerical simulation of piston ring lubrication. Tribology International, 41(9), 914-919.

1.4 The development of study lubrication with SPH

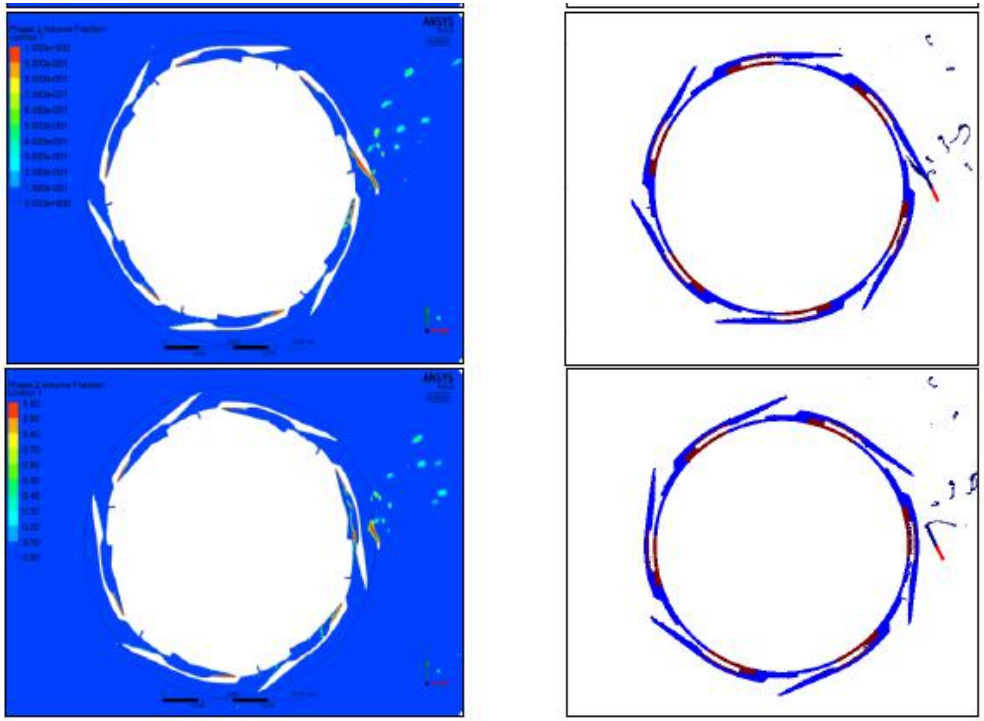

Fig. 5 Oil scoop

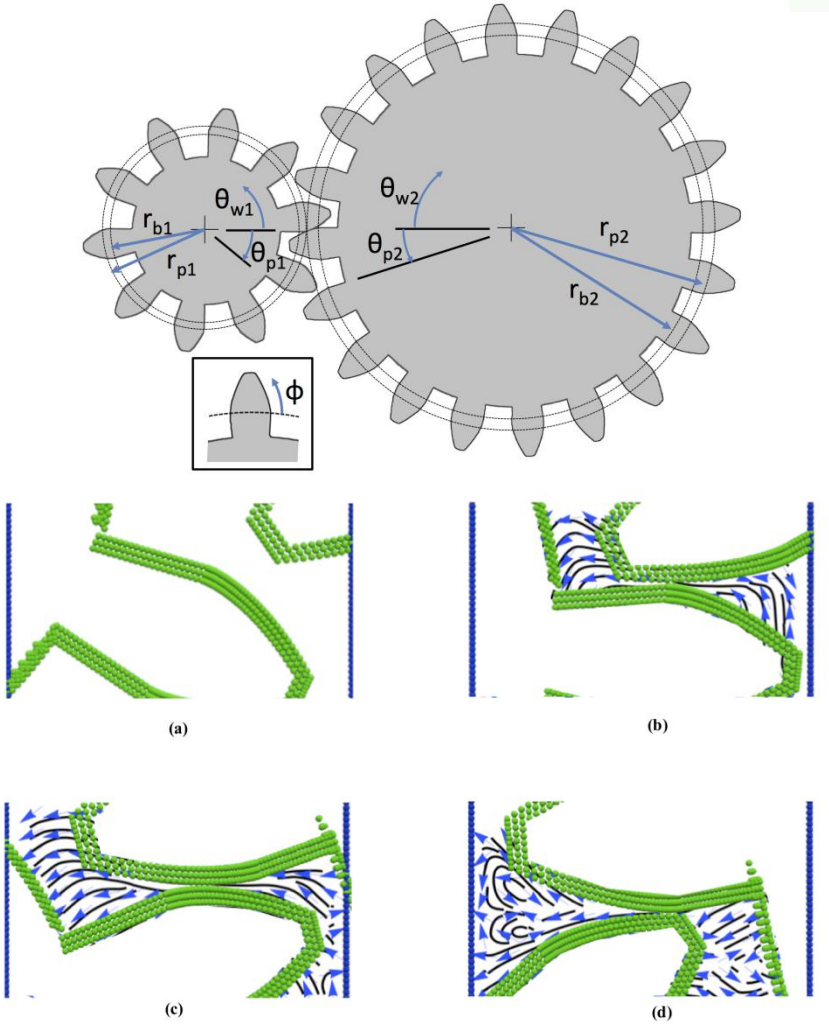

Fig. 6 Gear-Lubrication Study

[4] Korsukova, E., Kruisbrink, A., Morvan, H., Cageao, P. P., & Simmons, K. (2016, June). Oil Scoop Simulation and Analysis Using CFD and SPH. In ASME Turbo Expo 2016: Turbomachinery Technical Conference and Exposition (pp. V07BT31A027-V07BT31A027). American Society of Mechanical Engineers.

[5] Kyle, J. P. (2014). The Rheology of Nanoparticle Additives: An Investigation Utilizing Mesh Free Methods. Columbia University.

1.4 The development of study lubrication with SPH

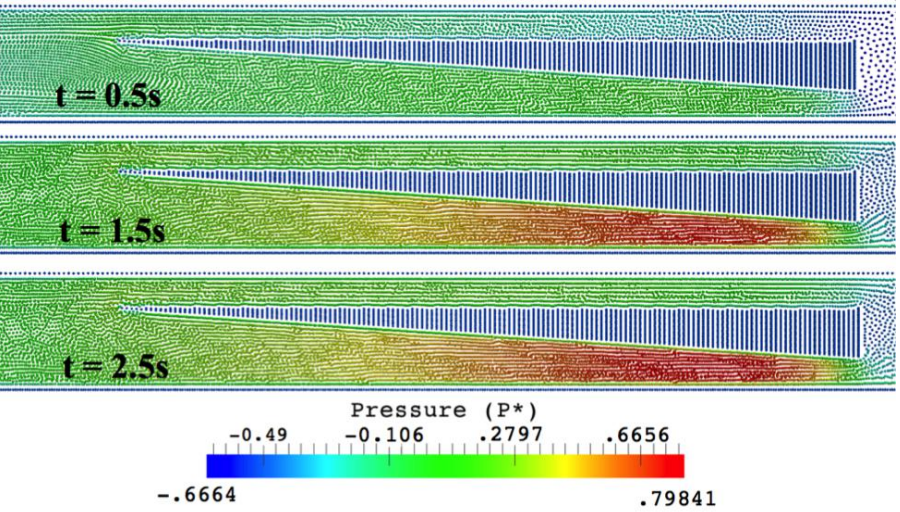

Fig.7 Full Film Lubrication

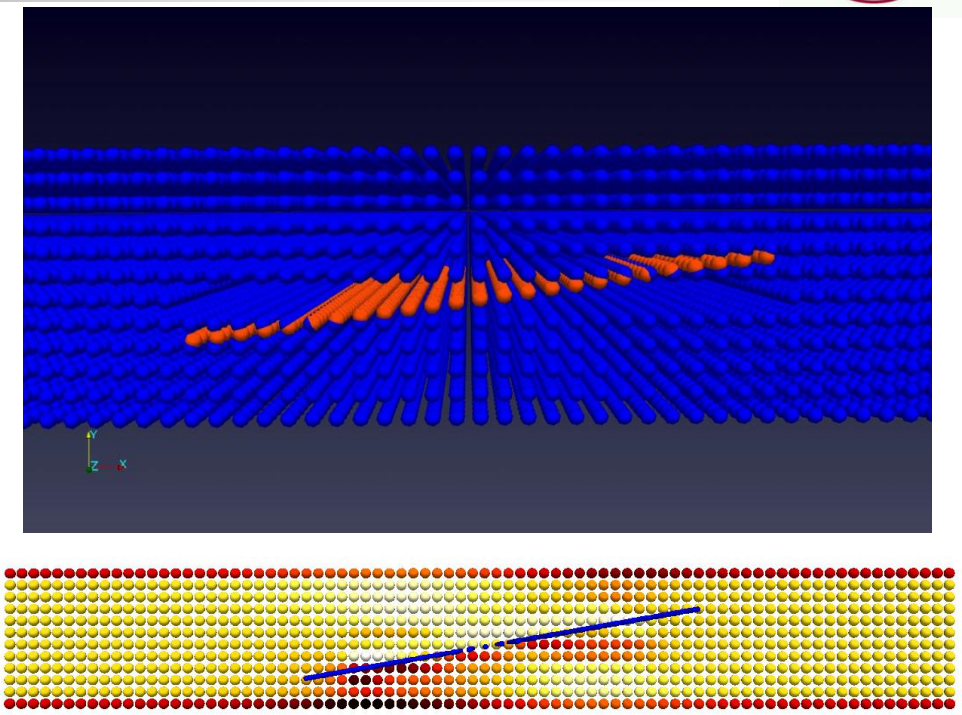

Fig. 8 Nanocomposite Lubrication

[5] Kyle, J. P. (2014). The Rheology of Nanoparticle Additives: An Investigation Utilizing Mesh Free Methods. Columbia University.

1.5 Summarize briefly

1) There is a large potential in improving the engine efficiency by reducing the friction between the piston skirt and the cylinder liner. It has great significance to study this problem.

2) The lubrication between the piston skirt and cylinder includes complex oil transport process, including splash, fracture and free surface evolution.

3) There are only limited studies about the lubrication have been done at different scales. It shows that SPH method can studied the lubrication phenomena in many ways, including the lubrication in internal combustion engine.

Contents

2.1 Theoretical source

Oil transport at the skirt-liner interface can be simplified as two simple models:

1) **Couette flow (shear flow)** which is driven by the viscous drag force and the inertia acting on the fluid due to the relative movement of the surfaces.

2) **Poiseuille flow (pressure flow),** which is driven by the pressure gradient.

Oil transport between the piston and the piston skirt is closer to the Couette flow.

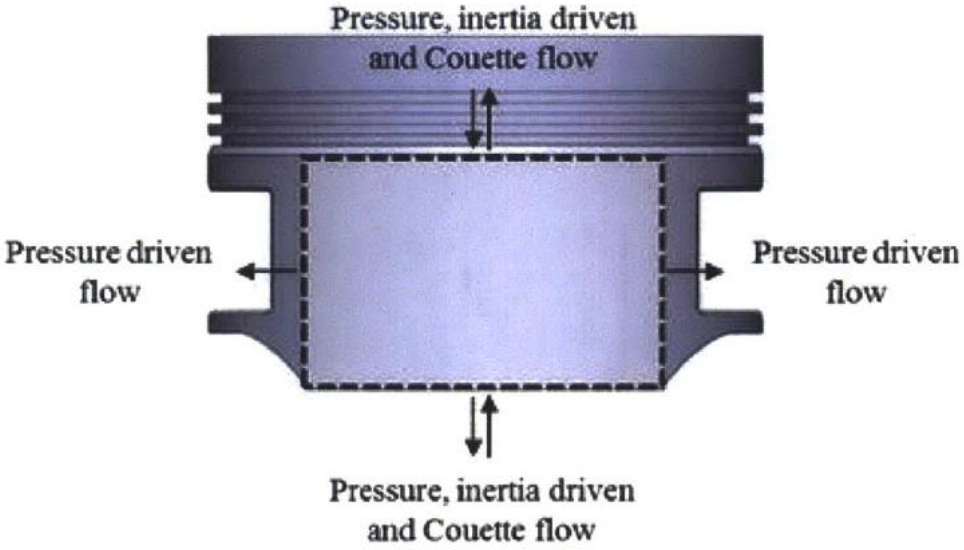

Fig.9 oil flow at the skirt's boundaries

[6] Kundu, Cohen, Dowling, "Fluid Mechanics", Academic Press, 2012.

[1] Bai D. Modeling piston skirt lubrication in internal combustion engines[D]. Massachusetts Institute of Technology, 2012.

[7] Totaro P P P. Modeling piston secondary motion and skirt lubrication with applications[D]. Massachusetts Institute of Technology, 2014.

2.2 model simplification

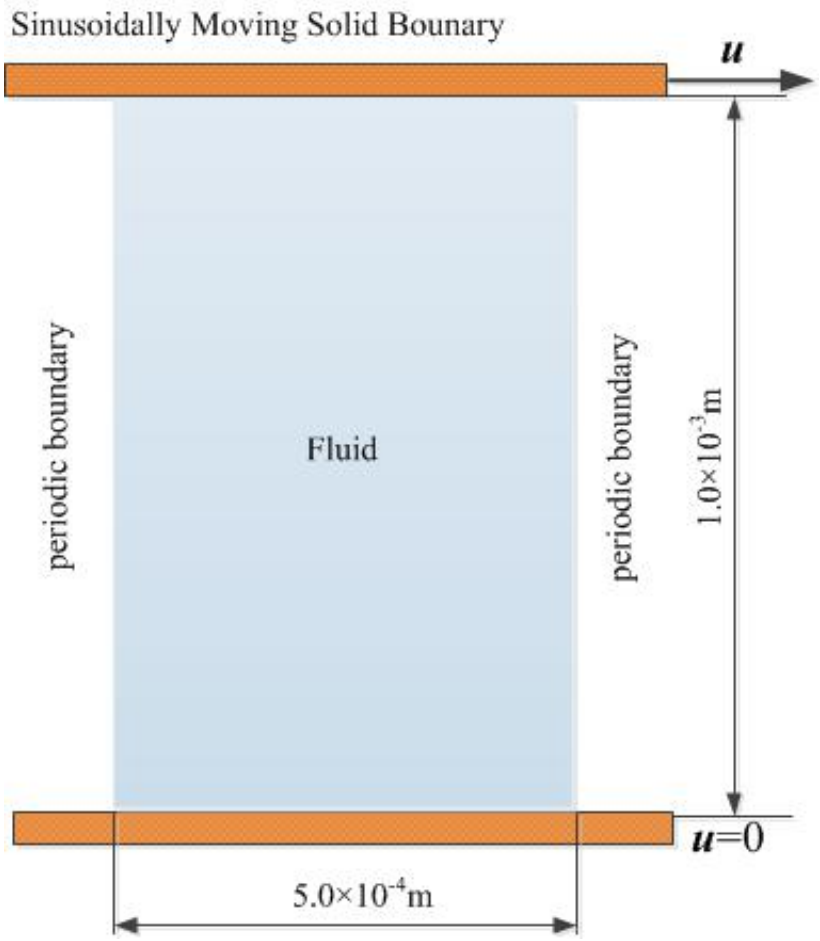

Fig. 10 Calculation Model

important parameters

$u = u_0 \times \sin 2\pi (ft+\theta)$

$f = R/60$

R rotational speed (r/min)

u_0 amplitude of the velocity

f frequency of velocity evolution

t time

T period of velocity change

θ initial phase

Y height of channel

μ 1.0×10^{-6}N·s/m² ~ 1.0×10^{-5}N·s/m²

u_0 1×10^{-4}m/s ~ 5.0m/s

t_{max} 25 T

f 10 Hz ~ 100 Hz

θ 0

ρ 800kg/m³

2.3 Simulation Method: SPH method

governing equations

$$\frac{d\rho_i}{dt} = \sum_j m_j \mathbf{v}_{ij} \frac{\partial W_{ij}}{\partial \mathbf{x}_i}$$

$$\frac{d\mathbf{v}_i}{dt} = -\sum_j m_j \left(\frac{p_i}{\rho_i^2} + \frac{p_j}{\rho_j^2} \right) \cdot \nabla_i W_{ij} + \sum_j \frac{m_j (\mu_i + \mu_i) \mathbf{r}_{ij} \cdot \nabla_i W_{ij}}{\rho_i \rho_j (\mathbf{r}_{ij}^2 + 0.01h^2)} \mathbf{v}_{ij}$$

Boundary Treatment

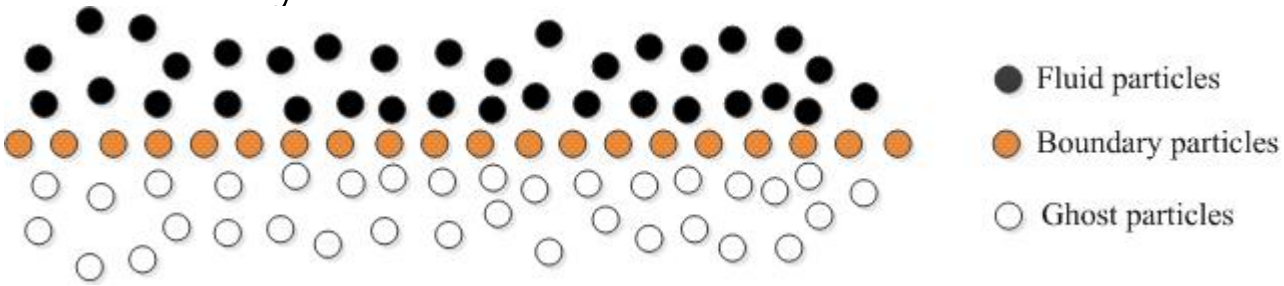

$$\begin{cases} x_g = 2x_w - x_i & y_g = 2y_w - y_i \\ v_{g,t} = v_{i,t} & v_{g,n} = -v_{i,n} \\ \rho_g = \rho_i \end{cases} \qquad p_g = \frac{\sum_j p_j W_{ij} \frac{m_j}{\rho_j}}{\sum_j W_{ij} \frac{m_j}{\rho_j}}$$

[8] Liu, G. R., Liu, M. B. (2003), Smoothed particle hydrodynamics: a meshfree particle method. World Scientific.

[9] Colagrossi, A., & Landrini, M. (2003). Numerical simulation of interfacial flows by smoothed particle hydrodynamics. Journal of computational physics, 191(2), 448-475.

Contents

3.1 Couette flow

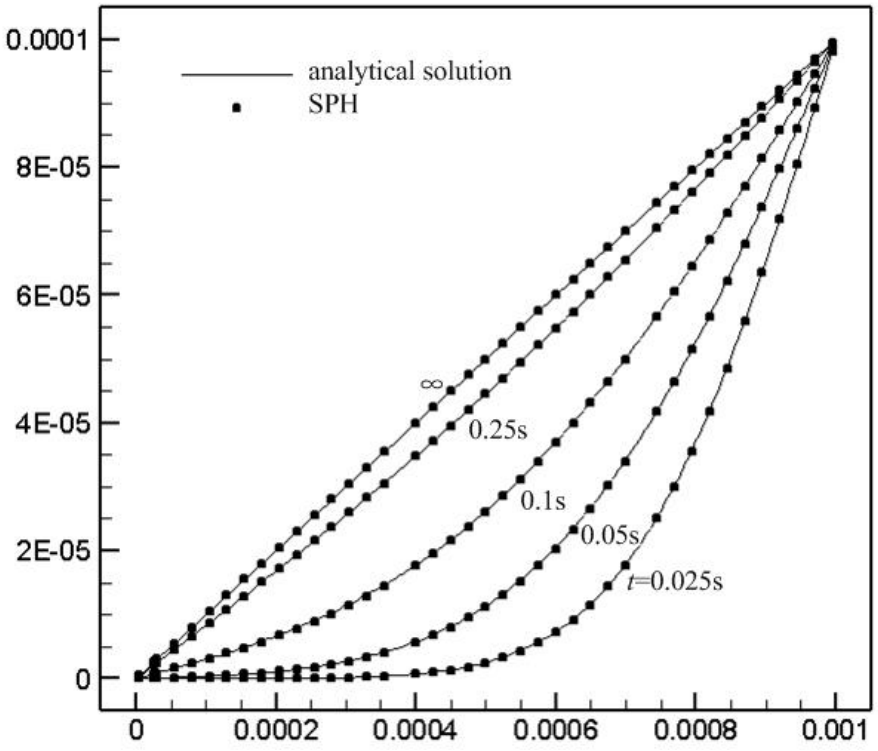

Fig. 11 Comparison of SPH and analytical solution.

The flow was simulated using SPH for $\mu=1.0\times10^{-6}$ N·s/m^2, $\rho=10^3$kg/m^3, $u_0=1.0\times10^{-4}$m/s. The results are in close agreement (within 0.2%), confirming the accuracy of the approach.

[10] Morris, J. P., Fox, P. J., & Zhu, Y. (1997). Modeling low Reynolds number incompressible flows using SPH. Journal of computational physics, 136(1), 214-226.

3.2 Effect of viscosity

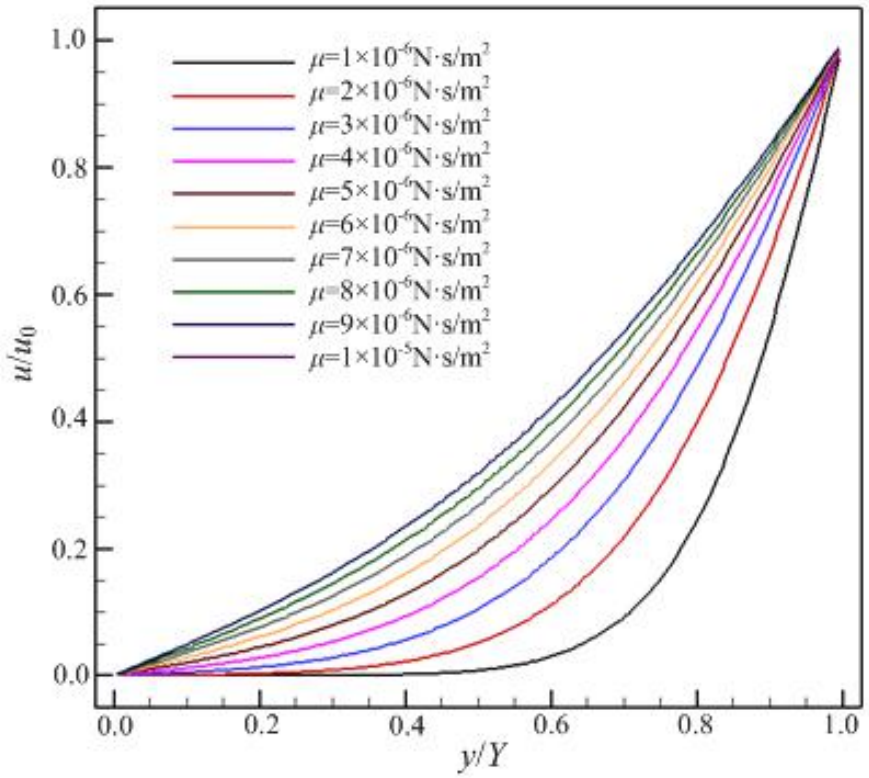

Fig. 12 Velocity of the vertical direction at f=10, u_0=1×10^{-4}m/s, t=T/4.

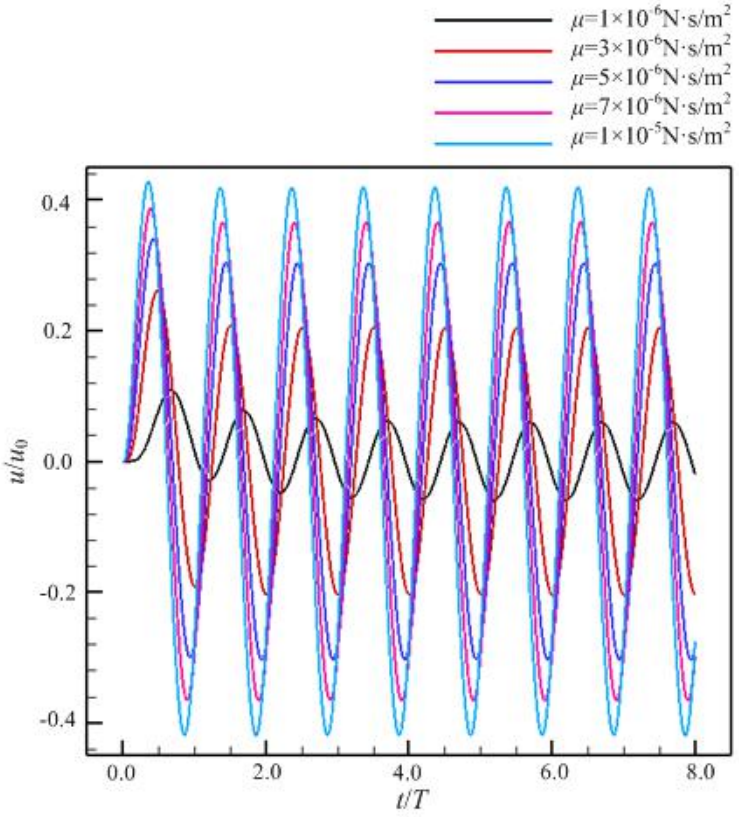

Fig. 13 Velocity change at Y/2 with time.

When the velocity amplitude is small and the velocity change frequency is constant, the viscous drag force plays a leading role in the oil transport process, and while the velocity is stabilized after two cycles.

3.2 Effect of viscosity

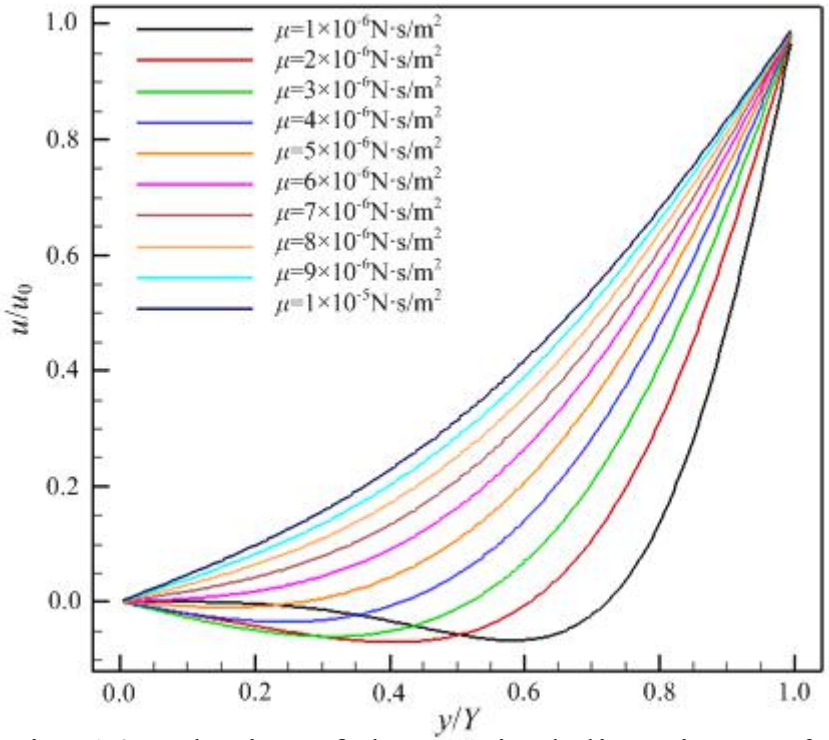

Fig. 14 Velocity of the vertical direction at f=10, u_0=1×10-4m/s, t=97T/4.

When the velocity variation frequency and the dynamic viscosity coefficient keep unchanged, the inertial force become more and more obvious with the increase of the velocity amplitude, while the speed is stable with more cycles.

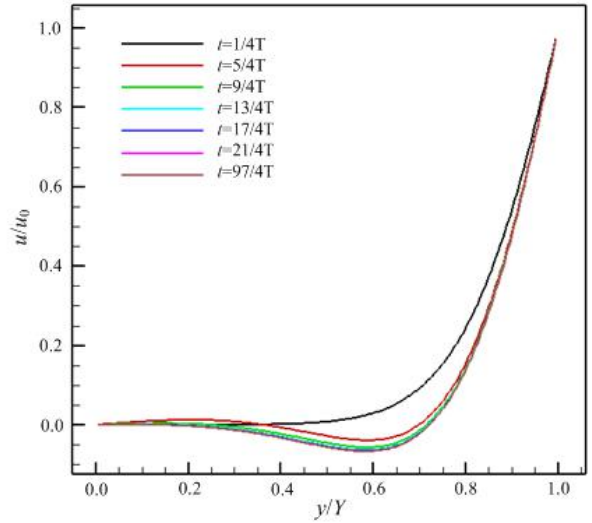

Fig. 15 Velocity of the vertical direction at μ=1.0×10-6N·s/m², different time.

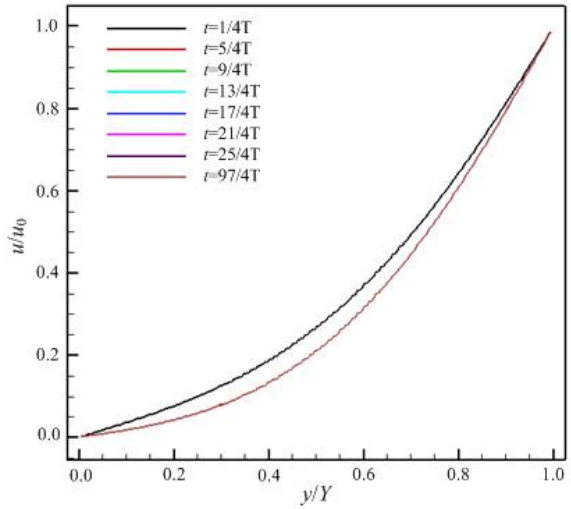

Fig. 16 Velocity of the vertical direction at μ=7.0×10-6N·s/m², different time.

3.3 Effect of frequency

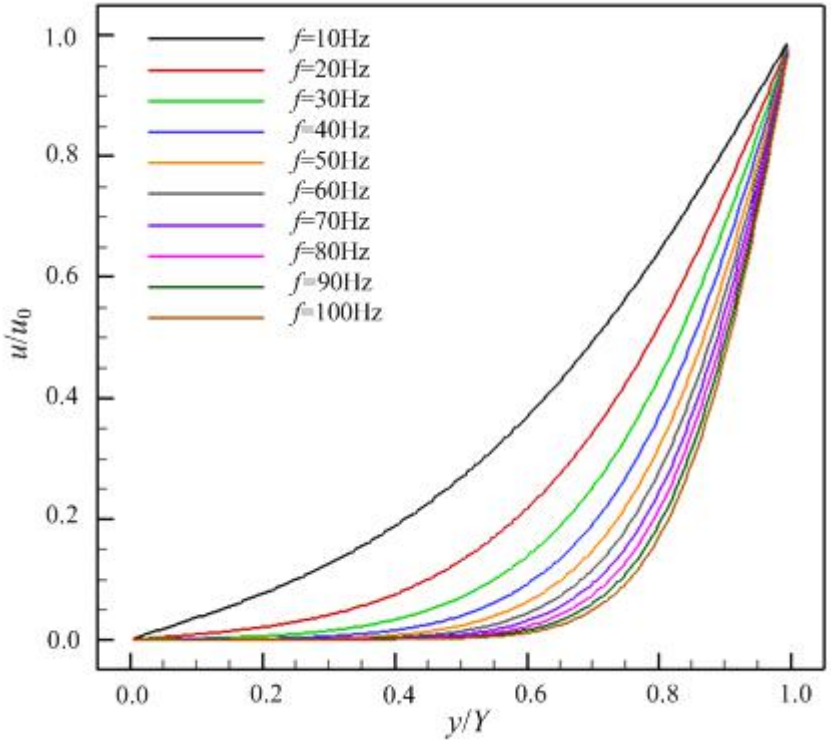

Fig. 17 The velocity distribution along the y-direction of calculation area at T/4 under different velocity change frequency, $\mu=7.0\times10^{-6}$ N·s/m^2, $u_0=1\times10^{-4}$m/s

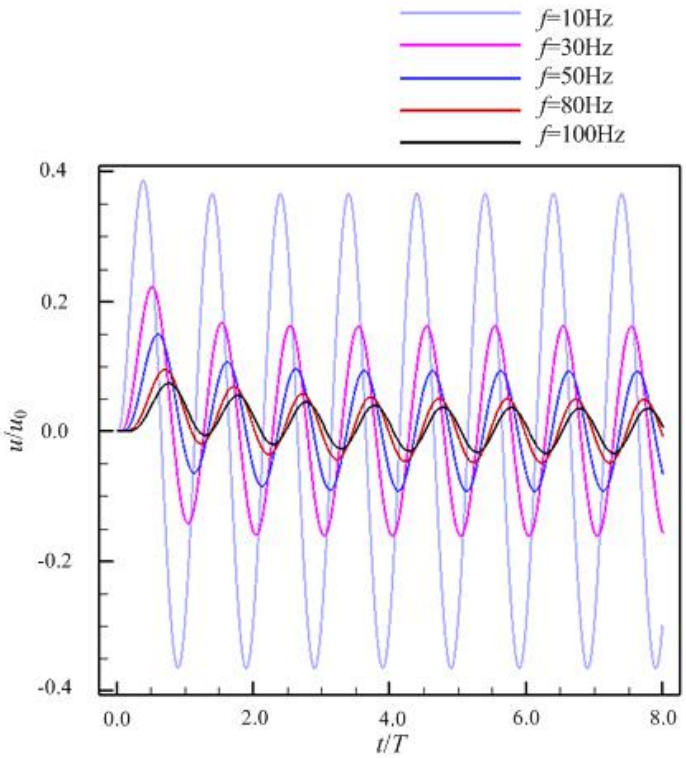

Fig. 18 Velocity change at $Y/2$ with time.

When the speed amplitude and the dynamic viscosity coefficient maintain constant, the inertial force become more and more obvious with the increase of the velocity variation frequency.

3.4 Effect of velocity

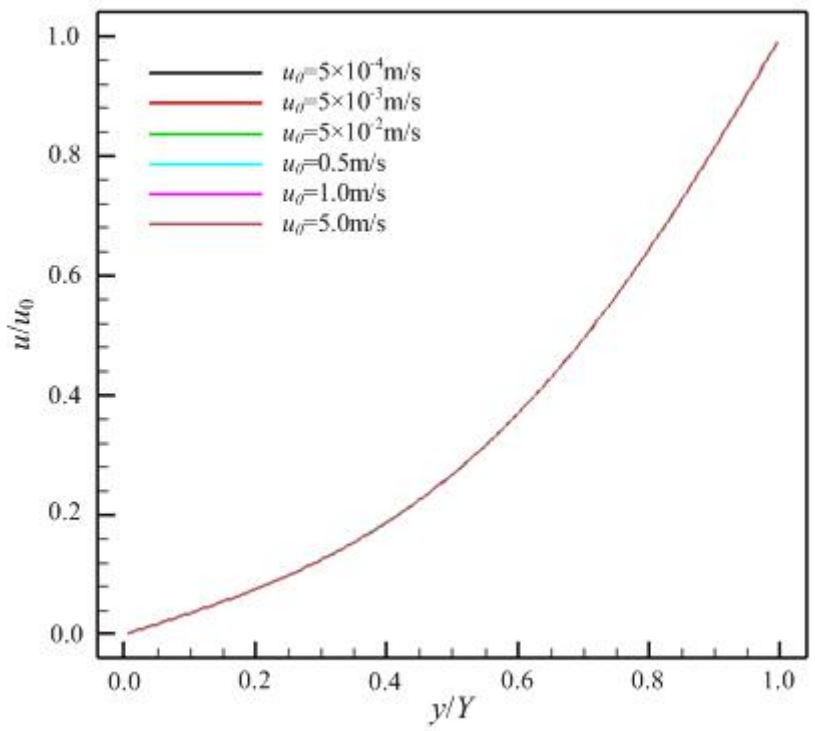

Fig. 19 Velocity of the vertical direction at f=10, μ=7.0×10^{-6} N·s/m^2, t=T/4.

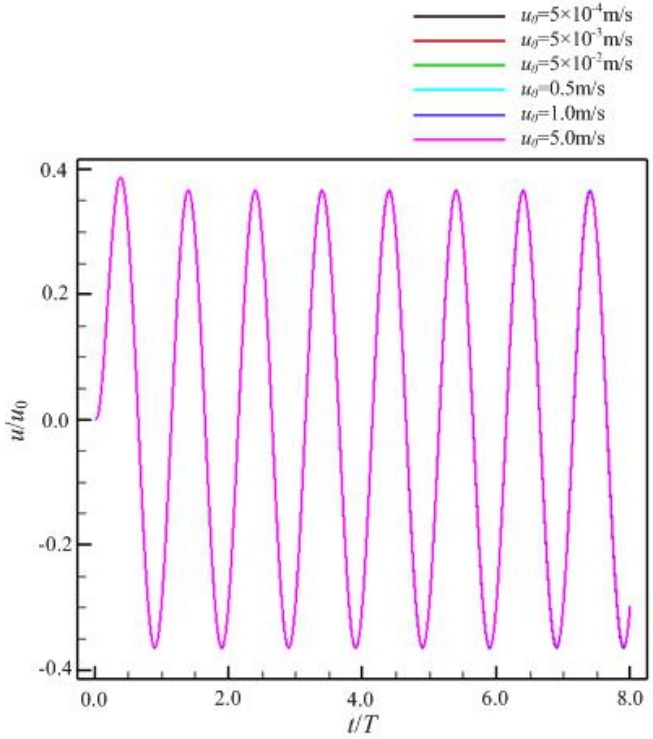

Fig. 20 Velocity change at Y/2 with time.

When the viscosity coefficient and frequency are constant, the velocity distribution is only related to the magnitude of the velocity amplitude, and is proportional to the vertical position.

3.5 Comprehensive Analysis

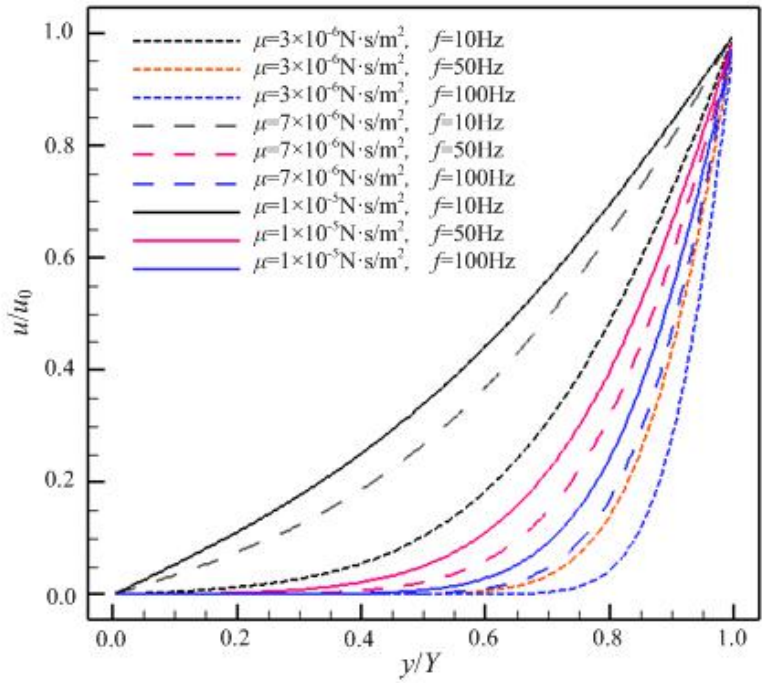

Fig. 21 Velocity of the vertical direction with different parameters

1) The viscosity of the oil plays a leading role of velocity distribution.
2) The velocity is close to the linear distribution with larger viscosity and smaller frequency, namely the viscous force plays a major role.
3) The Inertia force effect was significantly enhanced with smaller viscosity and greater frequency.

Contents

4 Conclusions

1) The SPH method is used to simulate the Couette flow under the sinusoidal period dragged speed for the first time.

2) The flow of the oil is related to many physical parameters under external drag force, and it is the most important parameters is dynamic viscosity.

3) It is try to choose an oil with smaller viscosity when the oil meet the lubrication requirements. In order to reduce the oil viscosity dissipation.

The end !

THANK YOU !